Friction Stir Brazing: a Novel Process for Fabricating Al/Steel Layered Composite and for Dissimilar Joining of Al to Steel

GUIFENG ZHANG, WEI SU, JIANXUN ZHANG, and ZHONGXIN WEI

A novel process of friction stir brazing (FSB) for fabricating Al/steel layered composite (by multipass) and for joining Al to steel (by single pass) was proposed to avoid the wear of pin by steel, in which a tool without pin was used. FSB of 1.8-mm-thick Al sheet to steel sheet was conducted using a cylindrical tool with 20-mm diameter but without pin and using 0.1-mm-thick zinc foil as filler metal. For the rotational speed of 1500 rpm, sound joints were reliably obtained at the medium range of traverse speed of 75 to 235 mm/min, which fractured within Al parent sheet during tensile shear test. Furthermore, for peel test on the sound joints, Al and steel parent sheets tended to crack and deform, respectively. Metallographic examination showed that most Zn was extruded and the resultant interfacial structure consisted of several Al-Fe intermetallic compounds (IMCs) with a little Zn, less than 3 at. pct. The thickness of IMCs can be controlled to be less than 10 μm by properly increasing traverse speed (*e.g.*, 150 mm/min). The metallurgical process of FSB was investigated by observing the microstructure of the longitudinal section of a friction stir brazed joint obtained by the suddenly stopping technique.

DOI: 10.1007/s11661-011-0677-0

I. INTRODUCTION

IT is well known that the fusion welding process is not applicable to dissimilar joining between aluminum and steel because of the formation of brittle intermetallic compounds (IMCs). Therefore, alternative joining processes in which no melting of both parent metals takes place (*e.g.*, brazing, roll bonding, and explosive welding) have been studied. Among them, furnace brazing[1,2] and rotational friction welding[3] were widely studied. For the preceding classical welding processes, joining time or temperature must be controlled carefully to be at low level to inhibit excessive thick IMCs formation.[2,3]

As a unique kind of energy source, laser beam provides some attractive advantages, including high power density, small heating area, rapid heating/cooling rate, and low heat input, which are beneficial in inhibiting the formation of IMCs. In recent years, several laser-assisted joining processes have received more attention; these include laser-assisted roll bonding,[4] laser pressure welding,[5] laser-induced reactive wetting without filler metal (only irradiating Al sheet to melt it),[6] laser brazing (only irradiating filler metal wire or steel sheet to melt filler metal by direct heating or heat conduction through the hot steel sheet),[7–9] and laser braze welding (irradiating both filler metal wire and Al sheet to melt and mix them).[10,11] For laser-assisted joining processes, shielding gas (argon)[6–11] or brazing flux (*e.g.*, fluor-base anticorrosive brazing flux[6–8,11]) is necessary, although satisfactory strength can be obtained by optimizing filler metal (*e.g.*, using Zn filler metal instead of the Al base one[9,10]) and process parameters.[8]

On the other hand, friction stir lap welding (FSLW) of Al sheet to steel sheet has also been attempted in recent years, because a joint is produced in solid state and no cover gas or flux is used.[12] In the case of joining Al to galvanized steel, strong joining could be readily achieved,[13–16] because the presence of Zn coating can produce the formation of a soft zone[13] or Al-Zn eutectic[14,15] at the bond interface, which contributes to the intimate contact or effectual mutual diffusion between the base metals. However, in most cases of joining Al to non-galvanized steel, there are some problems as follows. (1) The end of the pin will be damaged easily, because the pin tip must penetrate into the steel by 0.1 mm from the steel surface[13,17–19] to avoid the flat-bonded interface and rapid failure along the initial faying interface.[18] (2) IMCs also tend to form easily at the bond interface because of direct intermixing between Al and steel with intense plastic deformation.[13,17–21] (3) A few voids were observed along the interface and their size increased with increasing pin depth.[17,20]

Although the tool pin can be omitted to prevent wear in FSLW, the mechanical mixing between the top and bottom materials becomes difficult, resulting in very poor joint strength. For joining Al to dissimilar metals with relatively high hardness (such as steel, Ti, Cu, and stainless steel), the authors proposed a novel process of friction stir brazing (FSB) in which a tool without pin and filler metal must be used to avoid the severe wear of pin by hard parent metal and to induce metallurgical reaction instead of mechanically severe mixing between

GUIFENG ZHANG, Associate Professor, WEI SU, Graduate Student, and JIANXUN ZHANG, Professor, are with the State Key Laboratory for Mechanical Behavior of Materials, Xi'an Jiaotong University, Shaanxi Province 710049, People's Republic of China. Contact e-mail: gfzhang@mail.xjtu.edu.cn ZHONGXIN WEI, Senior Engineer, is with the Inspection Institute for Special Equipment, Guangxi Province 530022, People's Republic of China.

Manuscript submitted April 27, 2010.
Article published online April 2, 2011

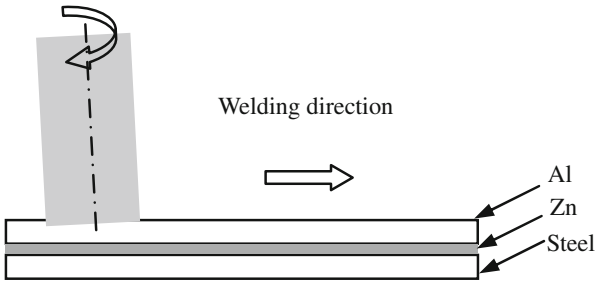

Fig. 1—Schematic diagram of FSB technique.

joining interfaces, respectively. Figure 1 shows the schematic diagram of the FSB technique.

As one of the friction stir processing[12,22,23] techniques, FSB should be a potential brazing process for fabricating layered composite without keyhole by multipass. Additionally, as a potential brazing process for Al and dissimilar metals with higher yield strength, FSB also offers several advantages over the traditional brazing process: no flux, shielding gas, or vacuum atmosphere; small expenditure of energy; and introduction of some mechanical actions (*e.g.*, forging[24–26] and torquing[27,28] actions) beneficial to eliminating oxide film and void defects.

The aim of the present study was to confirm the feasibility and repeatability of FSB of Al to steel by tensile shear test and by peel test and to investigate the final interfacial microstructure feature and some metallurgical processes in distinct stages or in distinct regions.

II. EXPERIMENTAL PROCEDURES

Commercially available pure aluminum sheet and low carbon steel sheet were used as base metals. Both of them were 1.8-mm thick, 100-mm long, and 6-mm wide. After polishing the surfaces to be joined by waterproof abrasive paper (grain size 400), the Al sheet was placed at the top and steel sheet at the bottom for lap joining. A commercial zinc foil with 20-mm width and 0.1-mm thickness was preplaced at the interface between the Al sheet and steel sheet. Zinc foil was chosen as the filler metal because of its low melting point of 693 K (420 °C), low eutectic temperature of 653 K (380 °C) with Al parent sheet, and good metallurgical compatibility with Al parent sheet (there is no intermetallic compound in Al-Zn binary system).

FSB was conducted on a conventional vertical milling machine in this study. A cylindrical tool made of medium carbon steel with a shoulder of 20-mm diameter, but without pin, was used, and the tool was tilted at 3 deg to enhance the forging effect of shoulder.[26] The plunge depth was manually controlled to be less than 0.5 mm. All samples were friction stir brazed at the same rotational speed of 1500 rpm. Only the traverse speed was varied as follows: 23.5, 75, 150, 235, 300, and 375 mm/min.

For each traverse speed, three joints produced at the same parameters were prepared for tensile shear test to demonstrate the feasibility and repeatability of the FSB process. Especially, considering that the FSB is not only a process for joining Al to dissimilar metal, but also a potential process for fabricating layered composite consisting of Al and dissimilar metal, three typical sound friction stir brazed joints for tensile shear test (produced at the traverse speed of 150 mm/min) were also evaluated by peel test. After the peel test, the fracture surface was analyzed using a scanning electron microscope (SEM) and X-ray diffraction to understand the fracture behavior during the peel test.

The metallographic examination was conducted on the cross section of the general friction stir brazed joint to investigate the relationship between tensile shear strength and traverse speed. Moreover, to more systematically explain the metallurgical process of FSB that took place in this system in distinct stages or distinct regions, the microstructure of the longitudinal section of a typical friction stir brazed joint obtained by the suddenly stopping technique (namely, suddenly retracting the tool and then stopping the forward motion of worktable[29]) was examined.

In the metallographic examination and mechanical property evaluation in this work, the terms advancing side and retreating side were defined as follows. The side of the weld where the local direction of the tool is the same as the traversing direction is called the "advancing side" (AS). The other side of the weld is called the "retreating side" (RS).[30]

III. RESULTS AND DISCUSSION

A. *Tensile Shear Property of Friction Stir Brazed Joints*

Figure 2 shows the appearance of as–friction stir brazed Al/steel layered composite produced by multipass FSB, demonstrating that the substrate of steel sheet can be readily clad with the sheathing of Al sheet in air and with low required energy (compared with vacuum roll bonding) and without a limit on the thickness of substrate sheet (compared with explosive welding). Figure 3(a) shows the appearance of a typical friction stir brazed joint produced at traverse speed of 150 mm/min by single-pass FSB. As expected, the weld beam surface was very smooth and no keyhole was observed in it. Figures 3(b) and (c) show the appearance of extruded Zn at the start and at the end of weld bead, respectively. Especially, at the end of the joint, Zn foil became greatly thick up to 0.5 mm from its initial thickness of 0.1 mm, which means that Zn foil can be preheated, melted, and extruded by the rotating and tilted shoulder.

Figure 4 shows the influence of traverse speed on the tensile shear failure load of the test sample with 25-mm width (slightly larger than the shoulder diameter of 20 mm) obtained with the same rotational speed of 1500 rpm. When the traverse speed was too low (*e.g.*, 23.5 mm/min) or too high (*e.g.*, 300 and 375 mm/min), the joint fracture load scattered greatly. In contrast, all joints obtained with medium traverse speeds of 75, 150, and 235 mm/min showed high fracture load with small scatter, and these joints fractured at RS within Al base

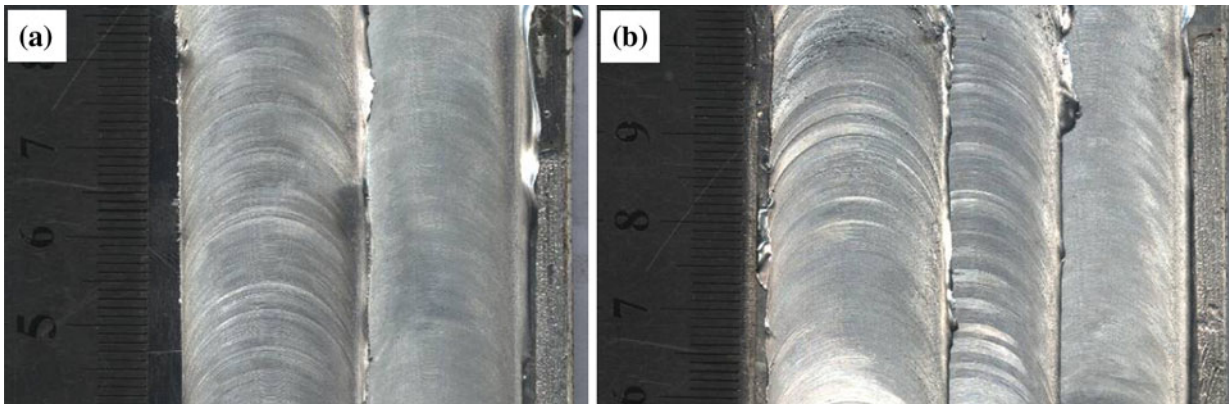

Fig. 2—Appearance of friction stir brazed Al/steel layered composite produced by multipass FSB: (*a*) 2 passes and (*b*) 3 passes.

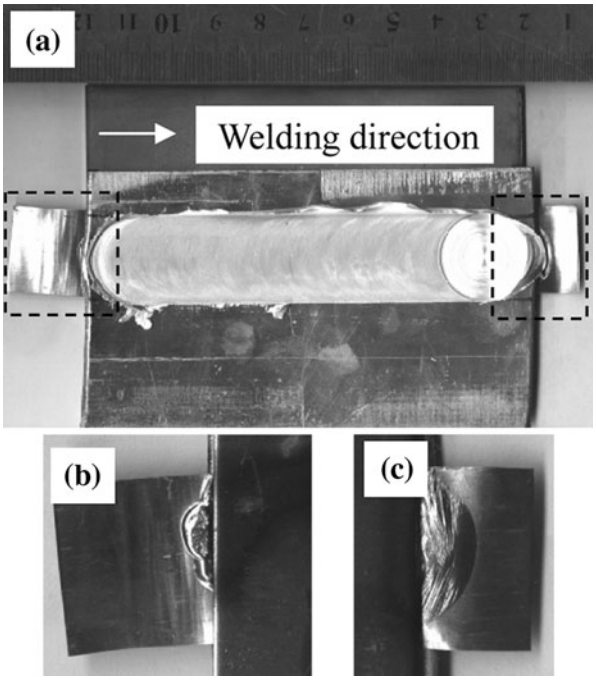

Fig. 3—Appearance of the (*a*) typical friction stir brazed joint and extruded Zn (*b*) at the start and (*c*) at the end of the weld bead.

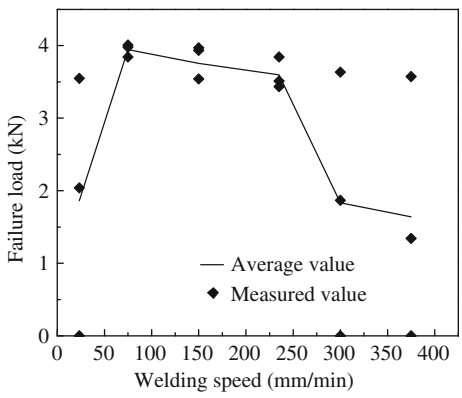

Fig. 4—Effect of traverse speed on tensile shear failure load of the friction stir brazed joints obtained with the same rotational speed of 1500 rpm.

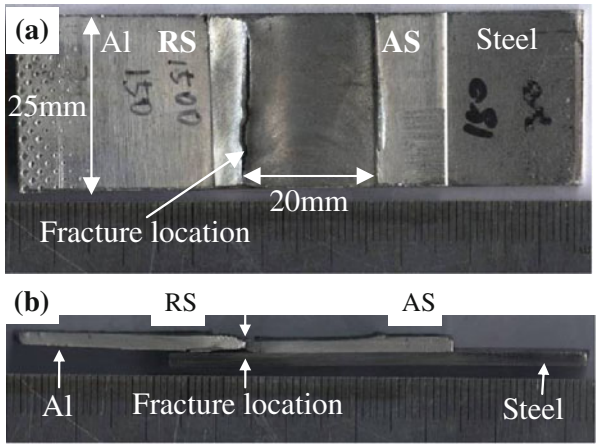

Fig. 5—Fracture location at RS within Al (but not along initial faying surface) after tensile shear test for a typical friction stir brazed joint produced at 150 mm/min × 1500 rpm.

metal, but not along the initial faying interface, as shown in Figure 5. The presence of the wide welding parameter window for sound joint demonstrated the feasibility and repeatability of the FSB process of Al to steel.

B. *Peel Test of the Typical Friction Stir Brazed Joints*

In order to investigate the interfacial joining strength of the friction stir brazed joints, three joints for peel test were produced under the same conditions (traverse speed of 150 mm/min and rotational speed of 1500 rpm), in which Zn foil was not preplaced over the entire interface, but was only preplaced at the second half interface, as shown in Figure 6(a). In this case, the heating behavior of Zn foil should be similar to that in the general FSB process, and the joints can be easily pre-peeled manually from the initial end (without Zn foil) to the central location (see the mark of "peel test start region" in Figure 6(a)) before peel test using a tensile test machine. The typical manually pre-peeled interface of the region without Zn foil filler metal is shown in Figure 6(b). For the peel test of the region with Zn filler, the three manually pre-peeled joints were further pulled by a tensile test machine at each separated end of the Al

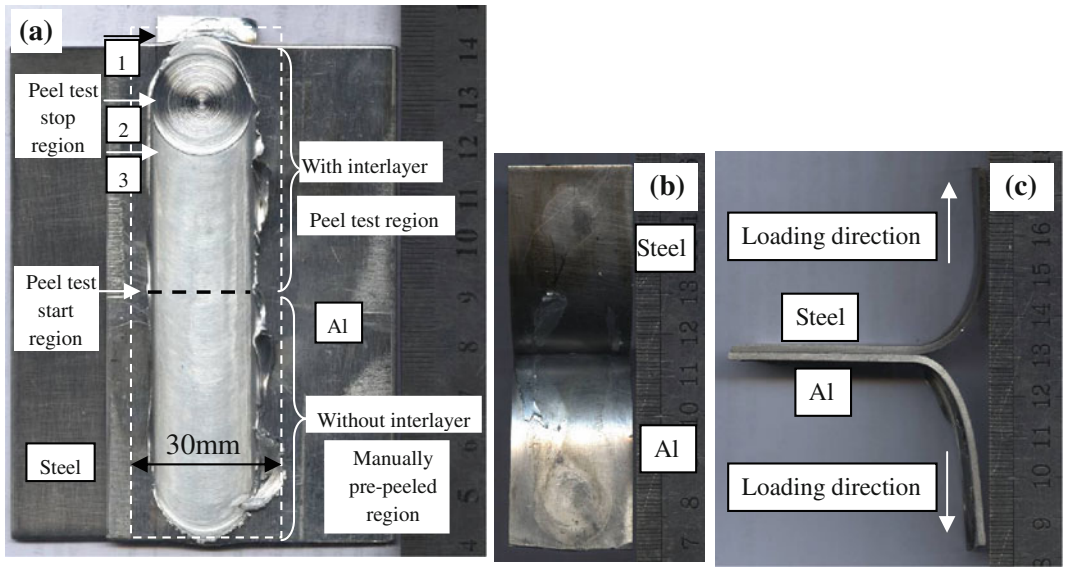

Fig. 6—(*a*) Appearance of the joint for peel test, (*b*) the manually pre-peeled fracture surface of the part without Zn foil filler, (*c*) and the part with Zn foil filler of the same specimen for further peel test using a tensile test machine.

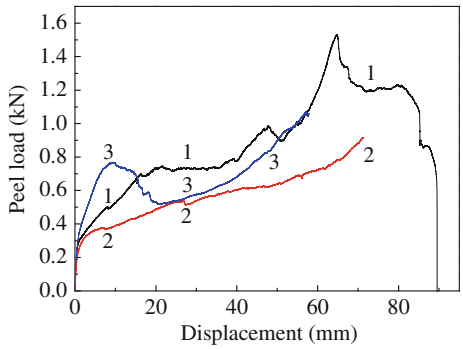

Fig. 7—Peel load-displacement curve of three samples produced under the same condition of 1500 rpm and 150 mm/min.

and steel sides (Figure 6(c)) to the "peel test stop position 1, 2, and 3" (Figure 6(a)), respectively; at the same time, the peel load was measured and recorded.

From Figure 6(b), it can be seen that at the region without Zn foil filler, neither adhered material (Al or Fe) nor interface deformation mark was observed on the smooth fracture surface. Both the high yield strength of steel and the high critical temperature required for diffusion of Fe atoms should be responsible for the poor interfacial bonding. The result also clearly demonstrated that it was hard to vertically mix Al and steel base metals only by forging and torquing actions of the tool shoulder, implying that a suitable filler metal with a eutectic temperature with Al below frictional heating temperature during FSLW (generally ~773 K (500 °C)) is required instead of difficult mechanical mixing for vertical bonding in the case of using a tool without pin.

Figure 7 shows the peel load-displacement curves of the three peel test joints. It should be noted that no significant and continuous decrease in peel loads was observed with increasing displacement for each specimen. The result suggested that there should be no crack in the bonded interfacial region. Furthermore, the peel load increased slowly with increasing the displacement, suggesting that the interfacial joining was so strong that a little deformation and resultant work hardening of the Al base metal would take place to a certain extent. In the middle region of displacement from 20 to 50 mm, the measured peel loads in curves 1 and 2 were 0.7 and 0.5 kN, roughly constant, respectively, which indicated that a stable peel was in progress, and the corresponding peel strengths were 35 and 25 N/mm, respectively.

Figure 8(a) presents the peeled appearance of the joint, which was stopped at the "stop position 3" in Figure 6(a). It is apparent that even the strong steel base metal was straightened from the initial "L" shape after peel test. Figures 8(b) and (c) present its fracture surface at low and high magnification, respectively, showing rough fracture surface with some macrocracks at the Al base metal side (especially at the area close to the root to be further peel tested) and some Al adhered at the steel side.

Figures 9(a) and (b) show the SEM micrographs of the fracture surface after peel test of the Al side and steel side shown in Figure 8(c), respectively. First, the most important information should be that a number of macro- and microcracks were observed at the Al side (arrows in Figure 9(a)), which means that the joint was so strong that even the Al base metal can be deformed and fractured during peel test. Second, the presence of the adhered materials (Al) at the steel side also revealed that the interfacial bonding between Al and steel was strong. Therefore, a sound Al/steel joint with favorable peel strength and fracture path during peel test can be obtained by the FSB process.

C. *General Microstructure of Friction Stir brazed Joints*

To understand the effect of the traverse speed on the failure load, the joint interfacial microstructures were

observed. Figure 10 shows the influences of traverse speed on the interfacial microstructure (backscattered electron (BSE) image) in the central region of the joint. From the color change in a BSE image (*e.g.*, Figures 10(a), (b), or (c)), the obtained interface layer was generally composed of 2 or 3 distinct IMC layers (Section D provides a detailed analysis). According to Figure 10, the influences of traverse speed on the thickness of IMCs in friction stir brazed joints can be summarized in Figure 11(a). It can be seen that the thickness of IMCs decreased with increasing traverse speed. When the traverse speed was too slow (*e.g.*, 23.5 mm/min), the resultant IMCs were too thick, more than 20 μm (sometimes a crack can be seen within IMCs), due to excessive heat input. While for too fast traverse speed (*e.g.*, 300 and 375 mm/min), although the formed IMC layer was very thin (3 to 5 μm), it was not continuous and uniform along the joint interface due to the lack of heat input, and so the intimate contact between two base metals was not completely achieved. For medium traverse speeds of 75, 150, and 235 mm/min, the formed IMC layers were continuous, roughly dense, and uniform because of proper heat input, and had a suitable thickness about 19, 8, and 6 μm, respectively, resulting in favorable repeatability in the tensile shear test. Moreover, as shown in Figure 11(b), the increase of the IMCs thickness with total heating time (obtained by dividing the shoulder diameter by welding speed) can be approximately described as the parabolic relation

$$\delta = 3.5 \cdot t^{1/2}$$

where δ is the thickness of IMCs (microns) and t is the total heating time (seconds).

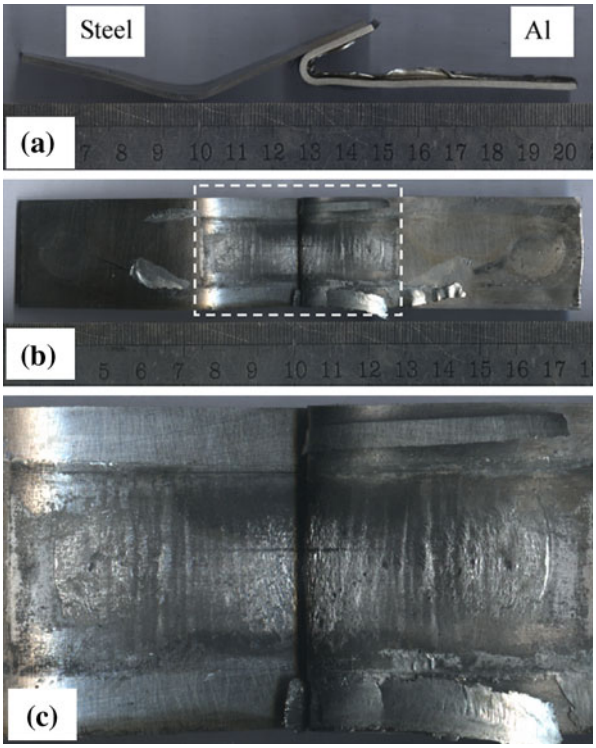

Fig. 8—Appearance of (*a*) the joint after peel test and the fracture surface subjected to peel test at (*b*) low and (*c*) high magnification.

D. *Macrostructure and Microstructure-Distribution Features of Joint Cross Section*

The typical structure of the joint produced at traverse speed of 150 mm/min is examined in detail in this section. Figures 12(a) and (b) show the joint macrostructure (BSE image) at RS and AS areas, respectively. Since the atomic number of Al, Fe, and Zn is 13, 26, and 30, respectively, the black, gray, and white region should be composed of Al, Fe, and Zn, respectively. It can be seen that a large amount of Zn filler metal was extruded and held at the region out of RS. The result shows that FSB has the advantage of extruding excessive filler metal with low melting point and low strength over conventional furnace brazing.

Figure 12(c) shows the microstructure-distribution features (BSE image) of the cross section of the same

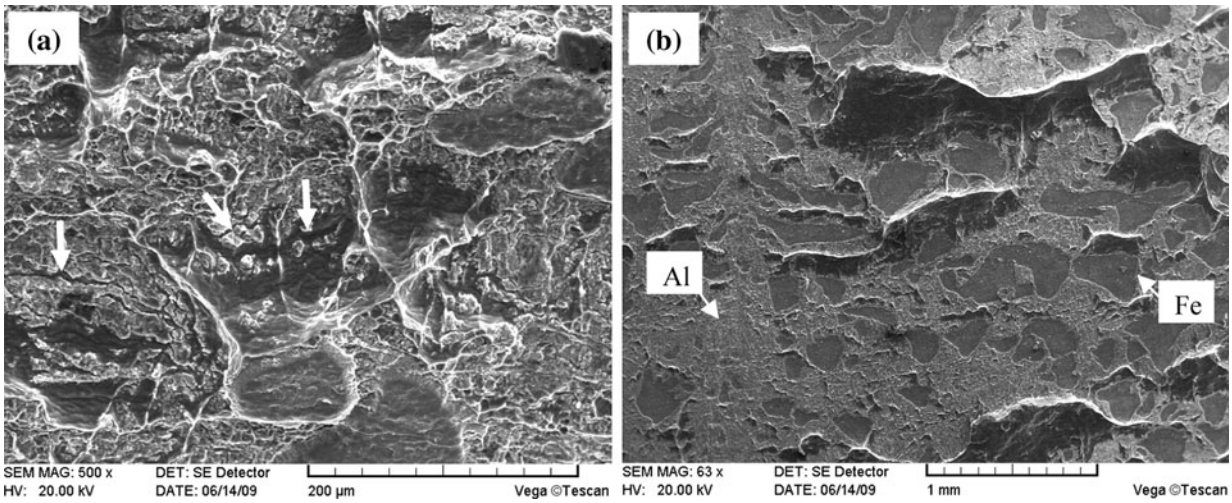

Fig. 9—SEM micrographs of the fracture surface after peel test shown in Fig. 8(c) at (*a*) Al side and (*b*) steel side.

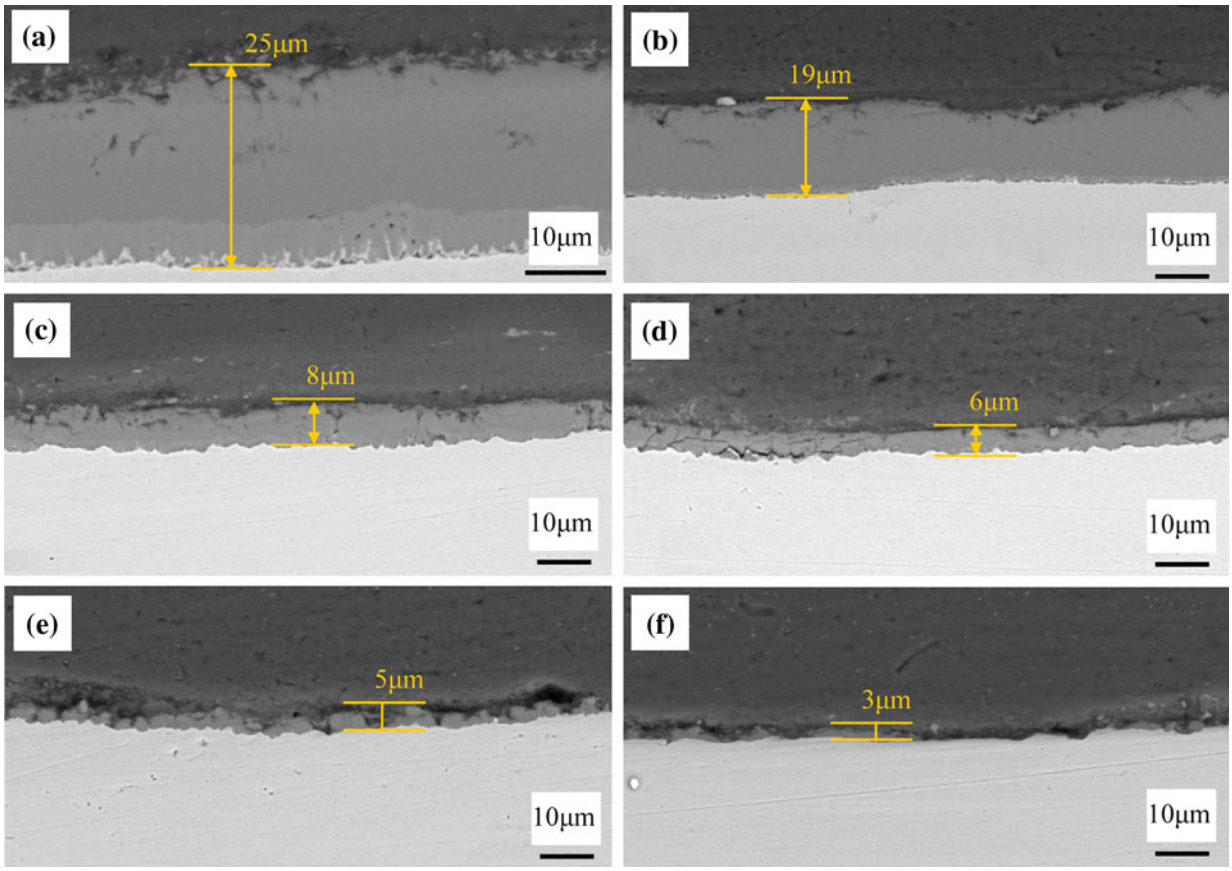

Fig. 10—Influence of traverse speed on microstructure and thickness of IMCs (BSE image): (*a*) 23.5 mm/min, (*b*) 75 mm/min, (*c*) 150 mm/min, (*d*) 235 mm/min, (*e*) 300 mm/min, and (*f*) 375 mm/min.

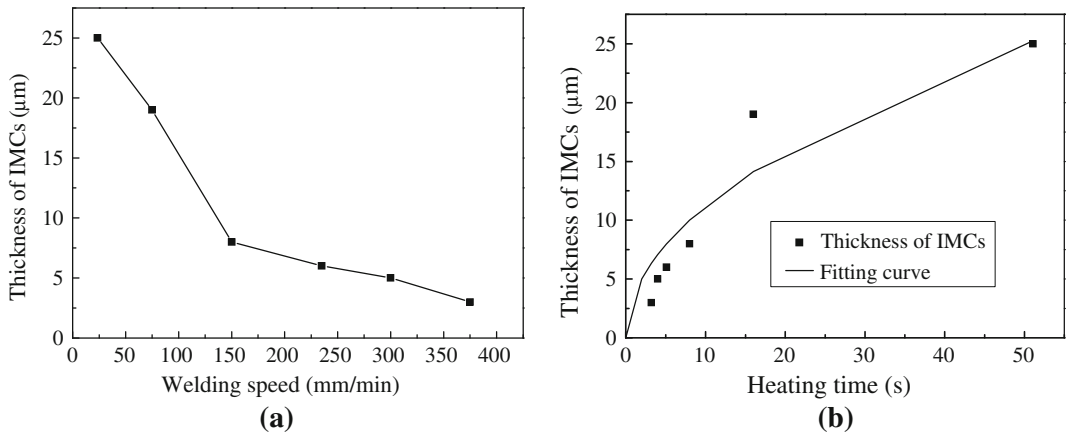

Fig. 11—Thickness of IMCs of friction stir brazed joints as a function of (*a*) traverse speed and (*b*) heating time (for the same rotational speed of 1500 rpm).

joint. Based on the distribution of Zn filler metal, the joint interface from the RS to central region can be divided into three regions: (1) region I (extruded Zn storage region), which was out of RS, holding extruded Zn filler metal; (2) region II (transition region), which was beneath the tool shoulder and at the boundary region of the braze seam inside RS, and where the thickness of residual molten Zn-Al alloy became gradually thin toward the center of the weld; and (3) region III (stable region), which has a roughly stable and uniform microstructure with little Zn toward the center, and has the greatest ratio to the interface to be joined (about 16 mm in width). The transition and stable regions were further examined in detail.

Figure 12(d) shows the BSE image of the "d" region within region II shown in Figure 12(c). From

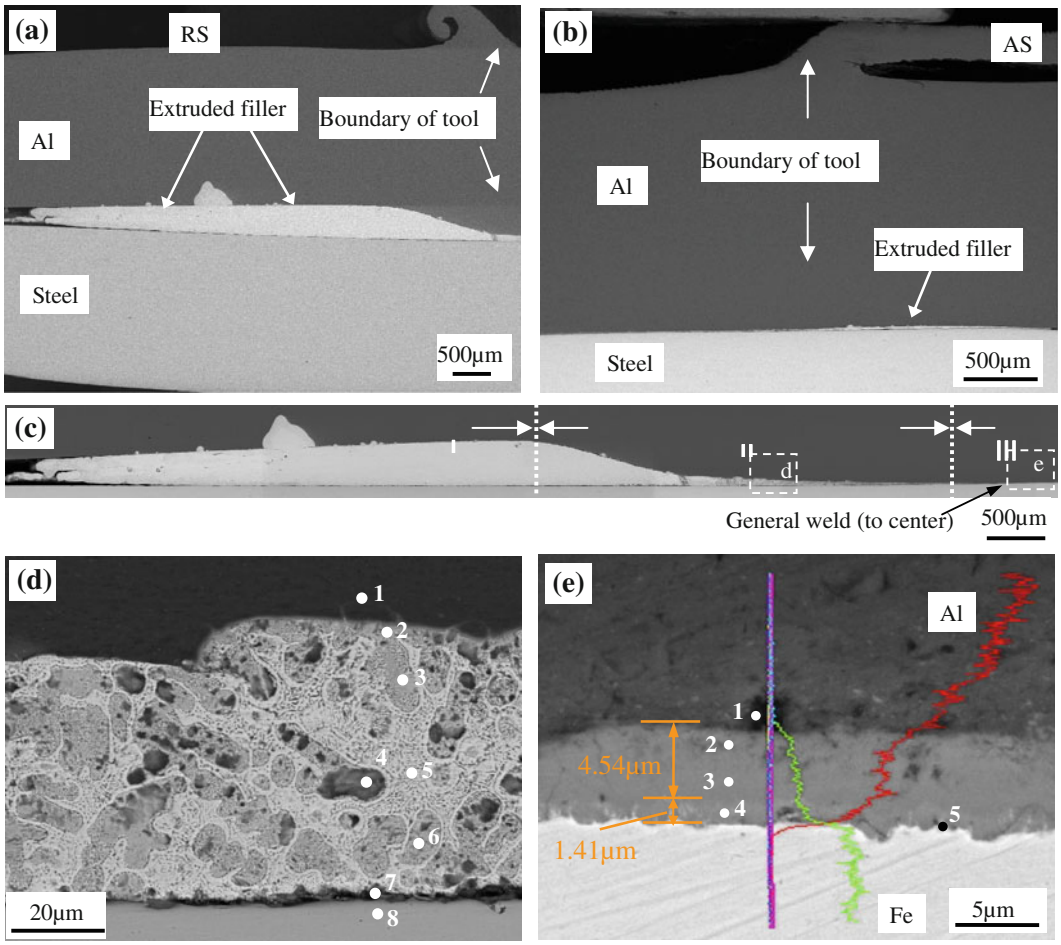

Fig. 12—Structure (BSE image) of cross section of the typical joint obtained with a traverse speed of 150 mm/min.

Table I. EDS Analysis Results in Distinct Regions Shown in Figs. 12(d) and (e)

Figure	Position	Elements (At. Pct) Al	Zn	Fe	O	Primary Element or Phase
12(d)	1	100.0	—	—	—	Al
	2	47.6	52.4	—	—	Zn and Al
	3	43.4	56.6	—	—	Zn and Al
	4	67.8	27.4	—	4.8	oxide
	5	10.5	89.5	—	—	(Zn)
	6	49.8	44.8	1.3	4.1	Al-Zn(Fe) alloy
	7	33.4	15.9	31.0	19.7	oxide
	8	—	—	100.0	—	Fe
12(e)	1	83.9	5.0	1.0	10.1	oxide
	2	80.1	2.5	17.4	—	$Fe_2Al_9(Zn)$
	3	74.7	1.5	23.8	—	$FeAl_3(Zn)$
	4	67.2	3.1	29.7	—	$Fe_2Al_5(Zn)$
	5	50.2	4.4	45.4	—	FeAl(Zn)

Figure 12(d) and the EDS point analysis result (Table I), the following important information can be obtained. (1) The Zn filler metal was completely melted, and quite an amount of Al base metal dissolved into molten Zn to form a Zn-Al alloy consisting of eutectic structure (being light gray, where the measured Al content at point 5 of 10.5 at. pct was close to the eutectic composition of 11.3 at. pct Al) and a supersaturated Zn-Al structure (being dark gray) containing a large amount of Al above 40 at. pct (points 2, 3, and 6 in Figure 12(d)) after relatively rapid solidification. (2) The continuous oxide film on the Al surface was successfully disrupted as dispersed particulate (below point 1 in Figure 12(e)) or trapped within liquid Zn-Al alloy as dispersed particulate (point 4 in the residual alloyed braze in Figure 12(d)). Therefore, clean and dense interfacial joining at the Al side was preferentially achieved more than on the steel side. (3) In contrast to the Al side interface, the oxide film on the steel surface remained continuously within region II. However, a little Fe was detected at point 6 (1.26 at. pct), showing Fe can dissolve into liquid Al-Zn alloy. Moreover, it should be noted that the surface of steel was covered by liquid Zn-Al alloy, but not pure liquid Zn. The presence of an amount of liquid Al should be beneficial to the wetting of alloyed braze on steel by the reduction reaction.

Figure 12(e) shows the microstructure (BSE) of region III. From the EDS line scanning and point

analysis results, it can be seen that there was little Zn in the interfacial layer (the detected maximum Zn content was less than 3 at. pct), while the interfacial layer consisted primarily of Al and Fe elements. Moreover, intimate contacts between the resultant interfacial layer and base metals were achieved at both Al and steel sides, although several black particles containing some oxygen (primarily consisting of Al and O) were observed at the Al side interface (which also demonstrated that the continuous alumina film was disrupted into dispersed particle with a size of about 2 to 3 μm). Furthermore, the difference in brightness of the BSE image of the residual interfacial layer showed it was composed of two distinct layers, although the composition profile was inhomogeneous at the boundary of the interfacial layer.

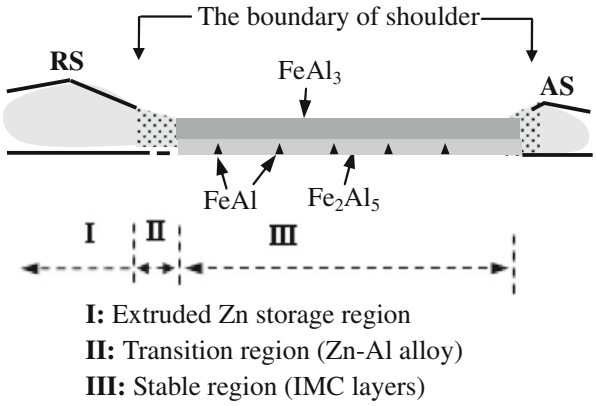

Fig. 13—Schematic diagram of the cross section of an friction stir brazed joint.

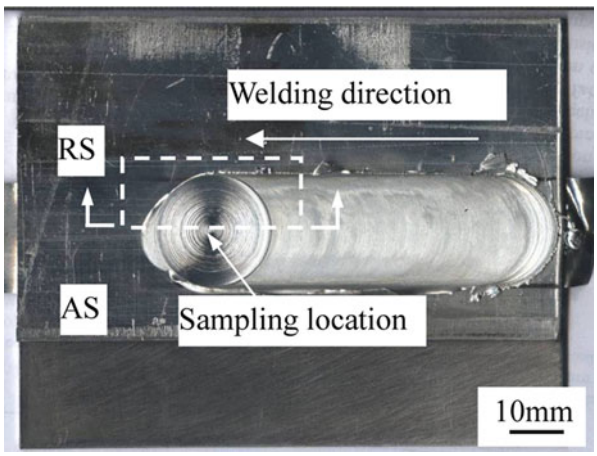

Fig. 14—Appearance and sampling location of the joint for suddenly stopped experiment.

Based on the EDS point analysis results at different layers and Al-Fe binary phase diagram, the IMC layer at the Al side with a thickness of about 4.5 μm should be primarily composed of $FeAl_3$(Zn) (point 3 in Figure 12(e)) with a small amount of metastable phase adjacent to Al such as Fe_2Al_9 (point 2 in Figure 12(e)). The second layer at the steel side should be Fe_2Al_5(Zn) with a thickness of 1.4 μm (point 4 in Figure 12(e)), in which a little Fe-rich phase of AlFe (Zn) showing white needle shape can be detected (point 5 in Figure 12(e)).

Figure 13 is a schematic diagram of the cross section of the typical friction stir brazed joint, showing various prominent microstructural features, namely, the extrusion of molten Zn, dissolution of Al, and the presence of IMC interfacial layers.

E. *Interface Evolution Behavior during FSB*

To understand the interface evolution behavior during FSB (such as the removal of oxide film, extrusion of liquid metals, and IMC formation), a suddenly stopped friction stir brazed joint was prepared by suddenly retracting the tool and then stopping the forward motion of the worktable. Figure 14 shows the appearance and sampling location for the suddenly stopped joint. Figure 15 shows its transitional portion in longitudinal sections from the front of shoulder to the location where stable microstructure consisting of continuous and dense IMC layers with a roughly constant

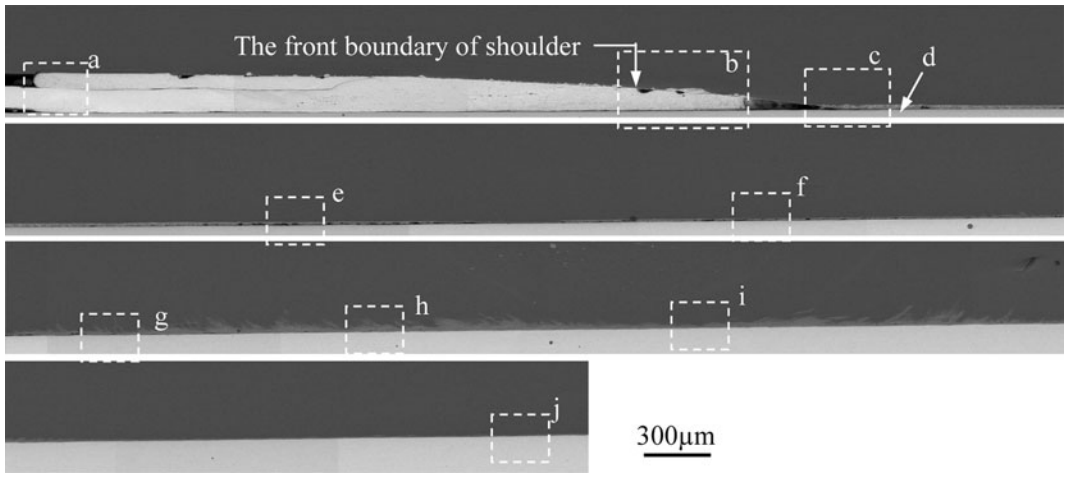

Fig. 15—Transitional portion in longitudinal sections (about 14 mm) of a suddenly stopped Friction stir brazed joint from the front of shoulder to the location where stable interfacial microstructure was present.

thickness (about 8.3 μm) was established. The transitional portion in longitudinal direction was about 14 mm in length and was completely beneath the shoulder of 20-mm diameter. Figures 16(a) through (j) show the several typical areas in Figure 15 at higher magnification. The transitional portion at the joint interface can be divided into four regions according to the interface evolution in distinct stages, as schematically shown in Figure 17.

Region I (extrusion of molten alloy, Figure 16(a)): In front of the shoulder, an additional layer present (gray) above the solid Zn (white) can be seen; and, according to the EDS line scanning result and its gray color in the BSE image, it should be extruded molten alloy mainly consisting of Zn and Al. The result also shows the presence of extrusion of excessive molten alloy and the dissolution of Al into molten Zn.

Region II (undermining of oxide film on aluminum and great dissolution of aluminum, Figures 16(b) through (d)): The evolution behavior of the interface at the Al side is shown in this region. In front of the shoulder, undermining[31,32] of the aluminum oxide film by molten Zn can be seen at several microzones, which allows dispersed oxide film to flow away. For example, at point 1 in Figure 16(b), the detected Al content was about 15 at. pct (Table II), slightly higher than eutectic composition. Moreover, as a result of undermining and the resultant dissolution of Al, the initial interface between Zn and Al completely disappeared and a liquid alloy with a hypereutectic composition (the detected maximum Al content reached about 60 at. pct; see points 4 and 5 in Figure 16(d)) was formed. According to the principle of transient liquid phase bonding, since Zn is a melting point depressant for Al, the molten Zn diffused into Al will result in a decrease in melting temperature of the Al substrate containing Zn. Therefore, the dissolution of Al into molten Zn (or widening of liquid zone[33]) takes place in appearance. Therefore, the removal of aluminum oxide film was preferentially achieved by undermining and subsequent great dissolution of Al to molten Zn.

Region III (partial wetting of steel by Zn-Al liquid alloy and slight dissolution of Fe and extruding molten alloy, Figures 16(d) through (f)): The evolution behavior of the interface at the steel side was shown in this region. From the EDS analysis result at points 4 and 5, it can be seen that the steel was covered by molten Zn-Al alloy, but not pure Zn. Thus, steel could be wetted partially with the aid of reactive Al in liquid state (Figure 16(e)). However, the lower heating temperature and short heating time will inhibit the reactive wetting. On the other hand, from the EDS analysis result at points 4 and 5, it can be seen that the slight dissolution of Fe into molten Zn-Al alloy has occurred. The feasibility of slight dissolution of Fe into molten Zn-Al alloy can be supported by the presence of a Zn-Al-Fe ternary eutectic reaction at 654 K (381 °C) and with a composition close to the Zn-Al binary eutectic composition (*i.e.*, Zn-11.3Al in at. pct) with a little Fe at the Zn-rich corner in Al-Fe-Zn liquidus projection, which implies that Fe can slightly dissolve into Zn-Al binary eutectic. Moreover, the molten alloy consisting of Zn, Al, and Fe was extruded, resulting in some voids preferentially present at the steel surface, which are to be eliminated by the forging action of the shoulder in the next region.

Region IV (initial generation, mixing, and growth of IMCs, Figures 16(f) through (j)): The formation behavior of interfacial IMC layers was shown in this region. With the forward motion of shoulder, in other words, with the enhancing of heating, stirring, and forging, the formation of IMCs can be analyzed in four distinctive stages: (1) initial generation of several separate IMC particles, (2) preferential connecting of IMCs along the surfaces, (3) upward mixing of small IMC particles assisted by enhanced stirring (while downward mixing was restricted by the strong steel), and (4) rapid growth and densification of IMC layers assisted by continuous frictional heating and enhanced forging at the trailing edge of shoulder. Finally, the formation of IMC layers with little Zn indicated that the FSB should be a diffusional process, rather than the *in-situ* solidification process of alloyed melt. It should be noted that the growth of IMCs occurs under the special conditions as follows: without liquid phase across the joint interface (Figures 16(e) through (j)), between the completely cleaned Al surface and partially cleaned steel surface, and with the aid of strong mechanical actions (torquing, forging, and the resultant stirring).[24–28] The observation of growth of IMCs also indicated that the diameter of shoulder should be an important factor affecting the thickness of interfacial IMCs, except rotational and traverse speeds. Since the mechanical and metallurgical phenomena and their coupling effect at the bond interface during FSB are invisible and complex, further study is needed to clearly characterize the interface evolution behavior (including the oxide film removal behavior at the steel side surface, dissolution behavior of Fe, upward mixing, and the entire formation process of stable IMC layers) and then to optimize the thickness of IMC layers.

For interface evolution behavior, the information obtained from the longitudinal section of the suddenly stopped friction stir brazed joint is quite consistent with that obtained from the cross section of a general friction stir brazed joint. According to these results, the metallurgical process of FSB that took place in this system can be more systematically explained as follows: undermining of the oxide film on Al substrate by molten Zn, significant dissolution of Al into molten Zn, slight dissolution of Fe into Zn-Al liquid alloy, extrusion of Zn-Al liquid phase with a little Fe, and the formation of IMC layers with little Zn by interdiffusion between Al and steel.

IV. CONCLUSIONS

1. For the typical friction stir brazed joint produced at traverse speed of 150 mm/min, the interfacial microstructure was found to be primarily composed of two distinct IMC layers (4.5-μm-thick $FeAl_3$(Zn) at the Al side and 1.4-μm-thick Fe_2Al_5(Zn) at the steel side), but the total thickness of the IMC layers was less than 10 μm. The Zn content in IMC layers was less than 3 at. pct. Moreover, the extruded

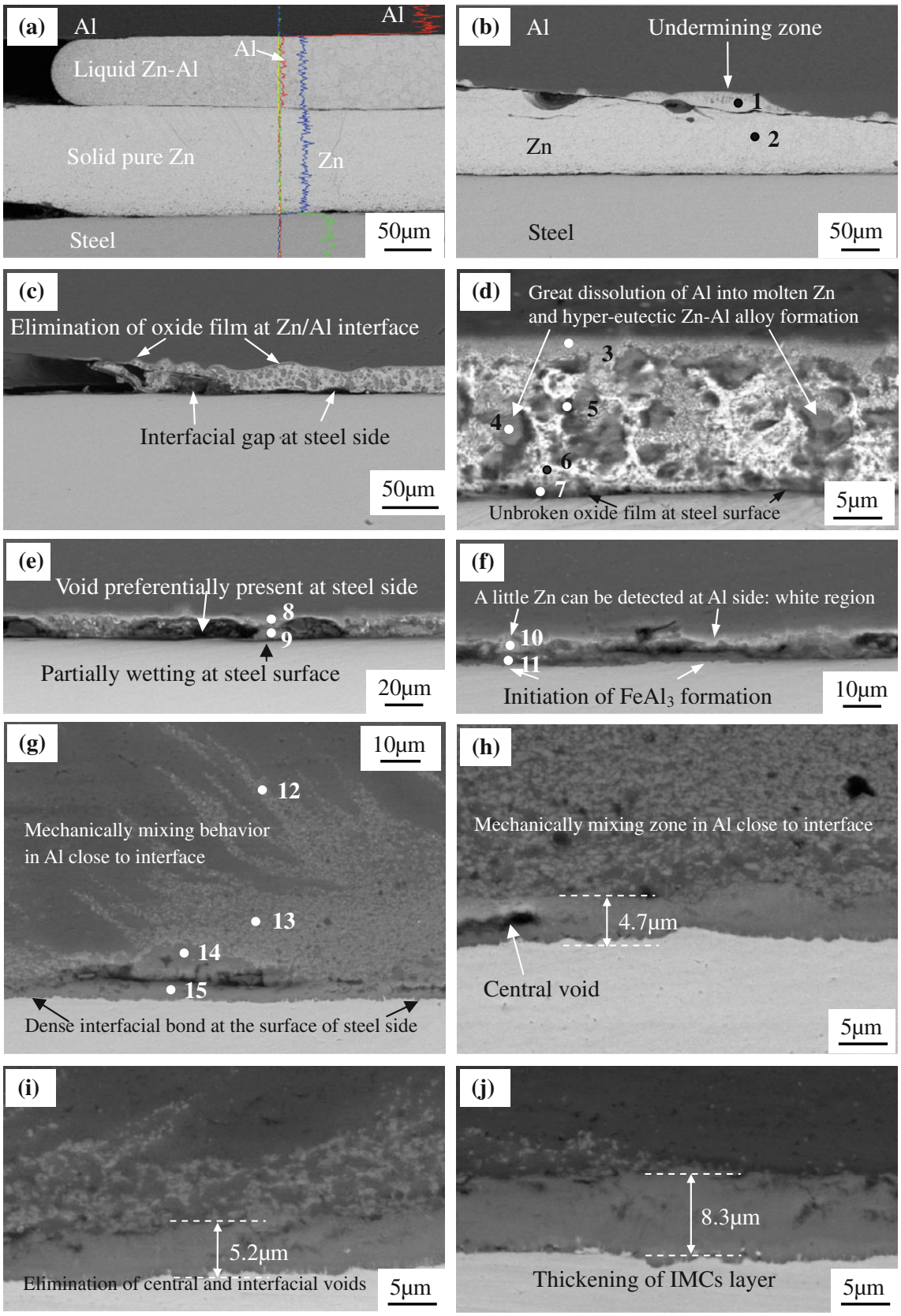

Fig. 16—Structure (BSE image) of longitudinal section of a suddenly stopped joint produced at 1500 rpm and 150 mm/min (the several typical areas shown in Fig. 15).

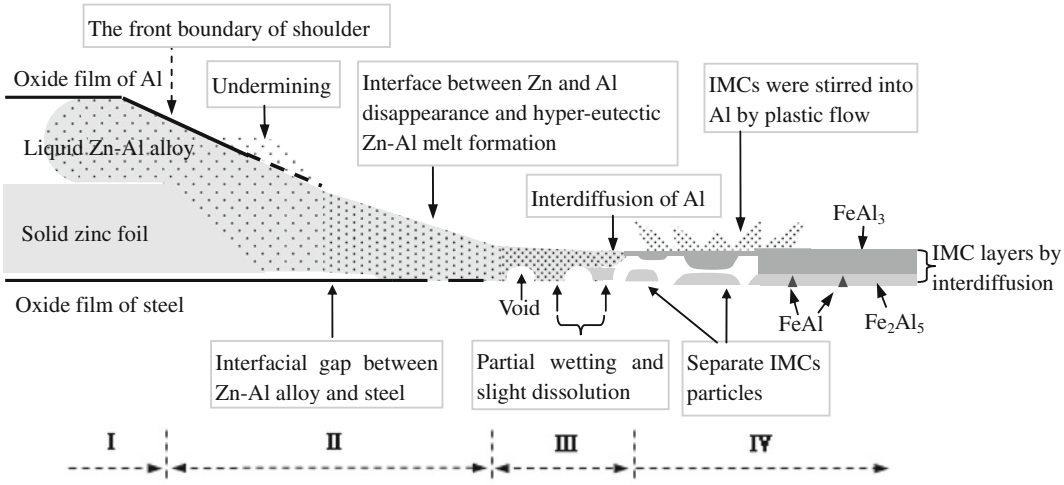

I: Extrusion of molten alloy

II: Undermining of oxide film on aluminum and great dissolution of aluminum

III: Partial wetting of steel by Zn-Al liquid alloy, slight dissolution of Fe and extruding molten alloy

IV: Initial generation, mixing and growth of IMCs

Fig. 17—Model of the formation of friction stir brazed joint.

Table II. EDS Analysis Results at the Locations Shown in Fig. 16

Locations	Zn	Al	Fe	O
1	84.3	15.6	—	—
2	96.9	3.1	—	—
3	24.8	74.7	0.5	—
4	27.0	66.4	1.4	5.2
5	30.4	60.1	0.8	8.7
6	74.4	15.9	4.2	5.5
7	56.3	28.5	5.0	10.2
8	19.4	77.9	0.9	1.8
9	20.9	71.9	1.8	5.4
10	20.0	75.3	1.8	2.9
11	7.5	64.7	21.8	6.0
12	3.6	87.7	8.7	—
13	5.2	79.4	15.4	—
14	8.9	87.1	1.8	2.2
15	5.2	66.4	23.2	5.2

liquid Zn-Al alloy at RS consisted of a eutectic structure and a supersaturated Zn-Al structure containing a large amount of Al over 40 at. pct. Therefore, great dissolution of Al into molten Zn was demonstrated.

2. According to the microstructure examination on the longitudinal sections of a suddenly stopped joint, the FSB process can be characterized by melting of Zn foil, undermining of the oxide film on Al substrate by molten Zn, significant dissolution of Al into molten Zn, slight dissolution of Fe into Zn-Al liquid alloy, extrusion of Zn-Al liquid phase with a little Fe, and formation of IMC layers with little Zn by interdiffusion between Al and steel. The excessive liquid phase was primarily extruded toward RS and the front of shoulder.
3. Intimate contact at the joint interface was well achieved by interdiffusion between base metals during FSB rather than the *in-situ* solidification of molten Zn-Al-Fe ternary alloy, instead of the plastic flow and vertical mixing for sound FSLW, to avoid wear of pin. With the aid of Zn foil and mechanical actions of shoulder, the oxide film on aluminum was preferentially removed by undermining, subsequent great dissolution of Al to molten Zn, and extrusion with liquid phase.
4. With increasing the traverse speed from 23.5 to 375 mm/min, the maximum thickness of IMCs decreased from 25 to 3 μm. When traverse speed was in the medium range of 75 to 235 mm/min, the interfacial IMCs had dense and continuous structure with proper thickness of 19 to 6 μm, and the joints fractured within Al base metal but not along the faying surface. The presence of the wide welding parameter window for sound joining confirmed the feasibility of FSB process.
5. During the peel test of typical sound joint produced at traverse speed of 150 mm/min, the peel load did not decrease with increasing the displacement, the Al base metal tended to cracking, and the steel was straightened from initial "L" shape after peel test. The actual peel strength can reach about 25 to 35 N/mm. Therefore, FSB may be a potential process for fabricating layered composite clad by Al.

ACKNOWLEDGMENT

This project was sponsored by the Scientific Research Foundation for the Returned Overseas Chinese Scholars, State Education Ministry.

REFERENCES

1. S. Liu, A. Suzumura, T.T. Ikeshoji, and T. Yamazaki: *JSME Int. J., Ser. A*, 2005, vol. 48 (4), pp. 420–25.
2. M. Roulin, J.M. Luster, G. Karadeniz, and A. Mortensen: *Weld. J.*, 1999, vol. 78, pp. 151s–155s.
3. K. Ikeuchi, N. Yamamoto, M. Takahashi, and M. Aritoshi: *Trans. JWRI*, 2005, vol. 34 (1), pp. 1–10.
4. M.J. Rathod and M. Kutsuna: *Weld. J.*, 2004, vol. 83, pp. 16s–26s.
5. K. Nishimoto, H. Fujii, and S. Katayama: *Sci. Technol. Weld. Join.*, 2006, vol. 11 (2), pp. 224–31.
6. P. Peyre, G. Sierra, F. Deschaux-Beaume, D. Stuart, and G. Fras: *Mater. Sci. Eng. A*, 2007, vol. 444 (1–2), pp. 327–38.
7. A. Mathieu, S. Pontevicci, J.C. Viala, E. Cicala, S. Matte, and D. Grevey: *Mater. Sci. Eng. A*, 2006, vols. 435–436, pp. 19–28.
8. K. Saida, W. Song, and K. Nishimoto: *Sci. Technol. Weld. Join.*, 2005, vol. 10, pp. 227–35.
9. T. Takemoto, S. Kimura, Y. Kawahito, H. Nishikawa, and S. Katayama: *J. Light Met. Weld. Construct.*, 2008, vol. 46 (7), pp. 8–16 (in Japanese).
10. A. Mathieu, R. Shabadi, A. Deschamps, M. Suery, S. Mattei, D. Grevey, and E. Cicala: *Opt. Laser Technol.*, 2007, vol. 39, pp. 652–61.
11. G. Sierra, P. Peyre, F. Deschaux-Beaume, D. Stuart, and G. Fras: *Sci. Technol. Weld. Join.*, 2008, vol. 13, pp. 430–37.
12. R.S. Mishra and Z.Y. Ma: *Mater. Sci. Eng. R.*, 2005, vol. 50, pp. 1–78.
13. A. Elrefaey, M. Takahashi, and K. Ikeuchi: *Q. J. Jpn. Weld. Soc.*, 2005, vol. 23 (2), pp. 186–93.
14. Y.C. Chen and K. Nakata: *Metall. Mater. Trans. A*, 2008, vol. 39A, pp. 1985–92.
15. Y.C. Chen, T. Komazaki, T. Tsumura, and K. Nakata: *Mater. Sci. Technol.*, 2008, vol. 24 (1), pp. 33–39.
16. Y.C. Chen, T. Komazaki, T. Tsumura, and K. Nakata: *Mater. Chem. Phys.*, 2008, vol. 111, pp. 375–80.
17. K. Kimapong and T. Watanabe: *Mater. Trans.*, 2005, vol. 46 (4), pp. 835–41.
18. S. Kumai, H. Sato, K. Suzuki, T. Ookawa, K. Lee, and M. Watanabe: *J. JILM*, 2007, vol. 57, pp. 529–35 (in Japanese).
19. M. Watanabe, T. Ookawa, and S. Kumai: *J. JILM,* 2007, vol. 57, pp. 536–41 (in Japanese).
20. K. Kimapong and T. Watanabe: *Mater. Trans.*, 2005, vol. 46 (10), pp. 2211–17.
21. L. Xing, L.M. Ke, and C.P. Huang: *Trans. China Weld. Inst.*, 2007, vol. 28, pp. 29–32 (in Chinese).
22. Z.Y. Ma: *Metall. Mater. Trans. A*, 2008, vol. 39A, pp. 642–58.
23. R.S. Mishra, Z.Y. Ma, and I. Charit: *Mater. Sci. Eng. A*, 2003, vol. 341, pp. 307–10.
24. C.J. Dawes and W.M. Thomas: *Weld. J.*, 1996, vol. 75 (3), pp. 41–45.
25. L. Cederqvist and A.P. Reynolds: *Weld. J.*, 2001, vol. 80 (12), pp. 281s–287s.
26. G.F. Zhang, W. Su, J. Zhang, and J.X. Zhang: *Sci. Technol. Weld. Join.*, 2011, vol. 16 (1), pp. 87–91.
27. G.F. Zhang, W. Su, J. Zhang, Z.X. Wei, and J.X. Zhang: *Trans. Nonferrous Met. Soc. China*, 2010, vol. 20 (12), pp. 2223–28.
28. A.P. Reynolds: *Scripta Mater.*, 2008, vol. 58, pp. 338–42.
29. K. Colligan: *Weld. J.*, 1999, vol. 78 (7), pp. 229s–237s.
30. P.L. Threadgill: *Sci. Technol. Weld. Join.*, 2007, vol. 12 (4), pp. 357–59.
31. Z.W. Xu, J.C. Yan, G.H. Wu, X.L. Kong, and S.Q. Yang: *Compos. Sci. Technol.*, 2005, vol. 65, pp. 1959–63.
32. W.F. Gale and D.A. Butts: *Sci. Technol. Weld. Join.*, 2004, vol. 9 (4), pp. 283–300.
33. I. Tuah-poku, M. Dollar, and T.B. Massalski: *Metall. Trans. A*, 1988, vol. 19A, pp. 675–86.